Molecular basis of selective resistance of the bumblebee BiNa$_v$1 sodium channel to tau-fluvalinate

Shaoying Wu[a,b], Yoshiko Nomura[b,c,d], Yuzhe Du[b,c,d,1], Boris S. Zhorov[e,f,g], and Ke Dong[b,c,d,2]

[a]College of Plant Protection, Henan Agricultural University, Zhengzhou, Henan, 450002, China; [b]Department of Entomology, Michigan State University, East Lansing, MI 48824; [c]Genetics Program, Michigan State University, East Lansing, MI 48824; [d]Neuroscience Program, Michigan State University, East Lansing, MI 48824; [e]Department of Biochemistry and Biomedical Sciences, McMaster University, Hamilton, ON, L8S 4K1, Canada; [f]Sechenov Institute of Evolutionary Physiology & Biochemistry, Russian Academy of Sciences, 194356, St. Petersburg, Russia; and [g]Institute of Molecular Biology and Genetics, Almazov Federal Heart, Blood and Endocrinology Centre, 197341, St. Petersburg, Russia

Insecticides are widely used to control pests in agriculture and insect vectors that transmit human diseases. However, these chemicals can have a negative effect on nontarget, beneficial organisms including bees. Discovery and deployment of selective insecticides is a major mission of modern toxicology and pest management. Pyrethroids exert their toxic action by acting on insect voltage-gated sodium channels. Honeybees and bumblebees are highly sensitive to most pyrethroids, but are resistant to a particular pyrethroid, tau-fluvalinate (τ-FVL). Because of its unique selectivity, τ-FVL is widely used to control not only agricultural pests but also varroa mites, the principal ectoparasite of honeybees. However, the mechanism of bee resistance to τ-FVL largely remains elusive. In this study, we functionally characterized the sodium channel BiNa$_v$1–1 from the common eastern bumblebee (*Bombus impatiens*) in *Xenopus* oocytes and found that the BiNa$_v$1–1 channel is highly sensitive to six commonly used pyrethroids, but resistant to τ-FVL. Phylogenetic and mutational analyses revealed that three residues, which are conserved in sodium channels from 12 bee species, underlie resistance to τ-FVL or sensitivity to the other pyrethroids. Further computer modeling and mutagenesis uncovered four additional residues in the pyrethroid receptor sites that contribute to the unique selectivity of the bumblebee sodium channel to τ-FVL versus other pyrethroids. Our data contribute to understanding a long-standing enigma of selective pyrethroid toxicity in bees and may be used to guide future modification of pyrethroids to achieve highly selective control of pests with minimal effects on nontarget organisms.

sodium channel | pyrethroids | tau-fluvalinate | bees | pyrethroid receptor site

Insecticides represent an essential component of global pest management programs against crop pests and vector-borne human diseases. However, insecticides also pose serious environmental and ecological risks, including potential harms to beneficial insects, such as bees, butterflies, and other pollinators that are critical for productivity in agriculture. Research on the effect of insecticides on bee species has intensified since 2006, with widespread honeybee colony losses, a phenomenon known as Colony Collapse Disorder (1). In addition to honeybees, bumblebees are important pollinators of many wild flowers in natural ecosystems (2). Similar to honeybees, bumblebees are commercially reared for the pollination of horticultural and agricultural crops (3, 4). Parallel to Colony Collapse Disorder in honeybees, significant declines in bumblebee populations have been reported (5–9).

Several major classes of insecticides, including neonicotinoids and pyrethroids, have been intensively investigated as one of the potential causes of Colony Collapse Disorder. Although these synthetic insecticide classes have been shown to possess relatively low mammalian toxicity (10), they are potentially toxic to non-targeted insects because of their broad-spectrum action on insect ion channels and receptors (10). In fact, the concern for off-target effects on beneficial insects has made discovery and deployment of selective insecticides one of the most important goals of modern toxicology and pest management research. Insecticides with a high toxicity against target insects, but a low toxicity to beneficial arthropods, would be ideal for implementation in integrated pest management programs. Research focused on enhancement of these qualities has led to the discovery of tau-fluvalinate (τ-FVL), which exhibits a highly selective toxicity profile. τ-FVL is a pyrethroid insecticide that belongs to a large class of synthetic compounds structurally derived from pyrethrins, which are the major insecticidal components of pyrethrum (i.e., dry flower extracts from *Chrysanthemum* spp.). Honeybees and bumblebees are highly sensitive to most pyrethroids, but they are less sensitive to τ-FVL (11, 12). Pyrethroids exert their toxic effects by disrupting the function of voltage-gated sodium channels, which are critical for electrical signaling in the insect nervous system. The effects of pyrethroids have been examined on sodium channels from the honeybee (*Apis mellifera*) in nerve preparations and the *Xenopus* oocyte expression system (13–17). Varroa mites (*Varroa destructor*), ectoparasites of honeybees, are more sensitive to τ-FVL than honeybees (18). As a result, τ-FVL is commonly used to control varroa mites in bee colonies in addition to other agricultural pests for crop protection (12).

The aim of this study is to elucidate the molecular basis of selective τ-FVL resistance in bumblebees. We cloned the sodium

Significance

Voltage-gated sodium channels are targeted by pyrethroids, which make up one of the largest classes of insecticides used globally for controlling human disease vectors and agricultural pests. Various pyrethroids can exhibit widely different toxicities on insect species. Most notably, bees are highly sensitive to most pyrethroids, but are resistant to tau-fluvalinate, a highly selective pyrethroid used to control varroa mites in beehives worldwide. However, the mechanism underlying bumblebee resistance to tau-fluvalinate remains elusive. Using mutagenesis, computer modeling of pyrethroid-receptor sites, and phylogenetic clues of sodium channel sequences, we uncovered bee-specific sodium channel residues that underlie species-specific pyrethroid selectivity. This finding could spur future development of a new generation of safer pyrethroids that selectively target pests, but not beneficial species.

channel, BiNa$_v$1–1, from the common eastern bumblebee, *Bombus impatiens,* and functionally characterized the channel in *Xenopus* oocytes. We discovered that the BiNa$_v$1–1 channel is highly sensitive to most pyrethroids examined, but resistant to τ-FVL. We found that three BiNa$_v$1–1 residues (T841 in IIS2, V926 in IIS5, and F1525 in IIIS6), which are conserved among sodium channels from bee species, are critical for the differential sensitivity of BiNa$_v$1–1 to τ-FVL versus other pyrethroids. F1525 and V926 are located in one of the two pyrethroid receptor sites, PyR1, whereas T841 is located outside of the pyrethroid receptor sites. Further computer modeling and mutagenesis uncovered four additional residues in the pyrethroid receptor sites that contribute to the unique selectivity of the bumblebee sodium channel to τ-FVL versus other pyrethroids. Our study establishes that receptor-site-dependent and receptor-site-independent residues in the BiNa$_v$1–1 channel contribute to the selective resistance of bumblebee sodium channels to τ-FVL, providing insight into the long-standing enigma of selective pyrethroid toxicity in bees. Knowledge gained from this study may be used to broadly guide future modification of pyrethroids to achieve highly selective control of pests with minimal effects on nontarget organisms.

Results

Molecular and Functional Characterization of the Bumblebee Sodium Channel BiNa$_v$1–1. We isolated a full-length sodium channel cDNA clone, *BiNa$_v$1–1*, from bumblebee brains, using RT–PCR. Similar to other voltage-gated sodium channels, the BiNa$_v$1–1 protein has four homologous repeat-domains, I–IV, each containing six transmembrane segments, S1–S6 (Fig. S1). All major sequence features that are critical for the function of sodium channels are conserved in BiNa$_v$1–1 (Fig. S1). Expression of the BiNa$_v$1–1 channel in *Xenopus* oocytes elicited inward sodium currents that were sensitive to inhibition by tetrodotoxin in two-electrode voltage-clamp experiments (Fig. S2A). The gating properties of BiNa$_v$1–1 (Fig. S2) are similar to those of the honeybee sodium channel AmNa$_v$1 (13) and other insect sodium channels (19–21).

We also cloned *BiTipE*, an ortholog of the *Drosophila TipE*, which encodes a sodium channel auxiliary subunit (22), and examined the effects of coexpression of BiTipE on the expression and gating of BiNa$_v$1–1 channels (Fig. S2 and Table S1). Similar to TipE, BiTipE enhanced the amplitude of peak currents of the BiNa$_v$1–1 channel. BiTipE did not alter the voltage-dependence of activation or inactivation of the BiNa$_v$1–1 channel (Fig. S2 B and C), but caused a depolarizing shift in the voltage dependence of slow inactivation (Fig. S2E). BiTipE had no effect on the recovery of slow inactivation (Fig. S2F).

Differential Sensitivities of the BiNa$_v$1–1 Channel to Different Pyrethroids. In voltage clamp experiments, pyrethroids typically prolong the opening of sodium channels, as indicated by the induction of large tail currents associated with membrane repolarization (23). Therefore, the amplitudes of pyrethroid-induced tail currents are a direct measurement of the potency of pyrethroids on sodium channels. Here we examined the sensitivity of the BiNa$_v$1–1 channel to two type I pyrethroids and five type II pyrethroids including τ-FVL (Fig. S3). Coexpression with BiTipE did not alter the sensitivity of the BiNa$_v$1–1 channel to pyrethroids, but enhanced amplitude of sodium currents, and was therefore used in all experiments.

Representative tail currents from all seven pyrethroids are shown in Fig. 1A. Strikingly, although large tail currents were induced by other pyrethroids at 1 μM, only small tail currents were induced by τ-FVL at the same concentration. As expected, the tail currents induced by type I pyrethroids permethrin and bifenthrin decayed rapidly, whereas the tail currents induced by the type II pyrethroids, deltamethrin (DMT), β-cyfluthrin, λ-cyhalothrin, and cypermethrin, decayed extremely slowly. As a type II pyrethroid, τ-FVL also induced slowly decaying tail currents, but only at a higher concentration (10 μM) (Fig. 1A).
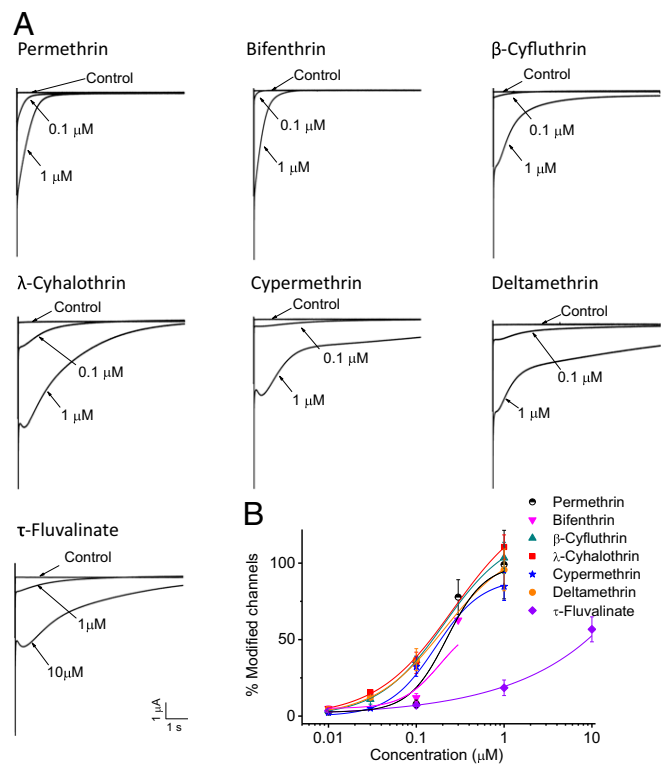

Fig. 1. Differential sensitivity of the BiNa$_v$1–1 channel to pyrethroids. (A) Representative tail currents induced by the seven pyrethroids. (B) Dose–response curves. Percentage of channel modification by pyrethroids was determined using the method by Tatebayashi and Narahashi (24). Dose–response curves were fitted to the Hill equation. EC$_{10}$, EC$_{20}$, and EC$_{25}$ values for τ-FVL are significantly different from those for the other pyrethroids (Table S2). The number of oocytes for each pyrethroid was >5. Each data point indicates mean ± SEM.

Next, we used amplitudes of pyrethroid-induced tail currents to quantify percentages of channels modified by insecticide following the method developed by Tatebayashi and Narahashi (24), yielding dose–response curves (Fig. 1B). The potency of each compound was compared using EC$_{10}$, EC$_{20}$, and EC$_{25}$ values (Table S2) because modification of only a small fraction of sodium channels is necessary to elicit symptoms of poisoning (25). The BiNa$_v$1–1 channel was more sensitive to type II pyrethroids than to type I pyrethroids. However, the BiNa$_v$1–1 channel was ca. 10- to 12-fold more resistant to τ-FVL than to type I pyrethroids, and 24- to 31-fold more resistant to the other type II pyrethroids based on EC$_{25}$ values. The sensitivity of BiNa$_v$1–1 channels to τ-FLV is significantly different from the sensitivity to other pyrethroids at EC$_{10}$, EC$_{20}$, and EC$_{25}$ levels.

Phenylalanine F[3i5(1525)] and Valine V[2o3(926)] Contribute to the Differential Sensitivity of BiNa$_v$1–1 to τ-FVL vs. Other Pyrethroids. Sodium channels from the German cockroach (*Blattella germanica*), the fruit fly (*Drosophila melanogaster*), and the yellow fever mosquito (*Aedes aegypti*) were more sensitive to τ-FVL than the BiNa$_v$1–1 channel (Fig. S4). We suggested that unique sequences in bee sodium channels might be responsible for this differential sensitivity. Homology modeling and mutagenesis predicted two pyrethroid receptors sites, PyR1 and PyR2, on insect sodium channels (19, 26). We scrutinized the sequences within and near PyR1 and PyR2 and found a phenylalanine residue, F1525 in IIIS6, which is conserved in sodium channels from all 11 bee species, including *A. mellifera* (Fig. S5). In contrast, at the corresponding position, a leucine is found in the sodium channels of all other 47 insect species with a

known sodium channel sequence including sodium channels from *B. germanica*, *D. melanogaster*, and *A. aegypti* (Fig. S5). Furthermore, a valine residue, V926 in IIS5, is also conserved in all bee species (Fig. S6). Interestingly, the sodium channel from varroa mites (*V. destructor*) has an isoleucine at the corresponding position, whereas sodium channels from all other insect species have either a valine or methionine, except for *Diachasma alloeum* and *Papilio machaon*, which also have an isoleucine (Fig. S6). To facilitate the comparison of sodium channels from different insect species, we used a nomenclature that is universal for sodium channels and other P-loop ion channels. In this nomenclature, each residue is denoted by the repeat number (1–4 instead of I–IV), segment type [k, S4–S5 linker; i, inner helix (S6); o, outer helix (S5)], and the relative position of the residue in the segment (27, 28). According to this nomenclature, F1525 is designated as F^{3i5} (i.e., F in the fifth position of inner helix IIIS6) and V926 as V^{2o3}. The label may also include the bracketed number of the residue in the protein sequence [e.g., $F^{3i5(1525)}$ and $V^{2o3(926)}$].

To determine the role of F^{3i5} and V^{2o3} in selective pyrethroid sensitivity, we substituted F^{3i5} with leucine and V^{2o3} with isoleucine in the $BiNa_v1–1$ channel (Fig. 2*A*). The F^{3i5}L substitution drastically reduced the sensitivity of $BiNa_v1–1$ channels to permethrin, bifenthrin, β-cyfluthrin, λ-cyhalothrin, cypermethrin, and DMT (Fig. 2*B*). However, the F^{3i5}L substitution did not alter the sensitivity of $BiNa_v1–1$ to τ-FVL (Fig. 2*B*). These results provide strong evidence that F^{3i5} contributes significantly to the sensitivity of the bumblebee sodium channel to most pyrethroids. In contrast, substitution of V^{2o3} with isoleucine significantly increased the sensitivity of $BiNa_v1–1$ channels to τ-FVL, but did not alter the sensitivity to other pyrethroids (Fig. 2*C*), suggesting that V^{2o3} plays a significant role in selective resistance of the bumblebee sodium channel to τ-FVL and that I^{2o3} in the varroa mite sodium channel could contribute to the sensitivity of varroa mites to τ-FVL. However, V^{2o3} is also present in $BgNa_v1$ channels that are sensitive to τ-FVL (Fig. S4), suggesting V^{2o3} is important for reduced τ-FVL sensitivity only in the context of the $BiNa_v1–1$ amino acid sequence.

T841 Outside PyR1 and PyR2 Contributes to $BiNa_v1–1$ Channel Resistance to τ-FVL. We then scrutinized the amino acid sequences of insect sodium channels for residues outside PyR1 or PyR2 that are conserved in bees, but not in other species. We found a threonine, T841, at the extracellular end of IIS2 in sodium channels of all 12 bee species, as well as in five species of ants and wasps (Fig. S7). In contrast, serine was found at the corresponding position in other insect sodium channels except for *D. alloeum*, which has isoleucine (Fig. S7). We substituted the threonine with serine in the $BiNa_v1–1$ channel and found that the mutant is more sensitive to τ-FVL, but less sensitive to permethrin, bifenthrin, β-cyfluthrin, λ-cyhalothrin, and DMT (Fig. 3), demonstrating that T841 contributes to differential sensitivities of τ-FVL versus other pyrethroids.

Docking DMT and τ-FVL in PyR1. In the PyR1 models (19, 29), which were built using the open potassium channel $K_v1.2$ as a template (30), F^{3i5} is located above residues V^{3i8} and I^{3i12}. In recent X-ray structures of open bacterial sodium channels NavAb (31) and NavMs (32), intersubunit fenestrations are much wider than those in $K_v1.2$. In the cryo-EM structure of the closed sodium channel, NavPaS (33), the II/III repeat interface is narrower than that in NavMs, but wider than in $K_v1.2$ (Fig. S8). A recent NavMs-based model of the open Nav1.4 channel is consistent with experimental data on the action of very different ligands that target the pore domain (34). Therefore, in this study, we have built a NavMs-based model of the open $BiNa_v1–1$ channel and used the ZMM docking methodology (19, 35) to predict possible binding modes of DMT and τ-FVL in PyR1. Initially, we imposed distance constraints between DMT and two residues, F^{3i5} and M^{2k11}.
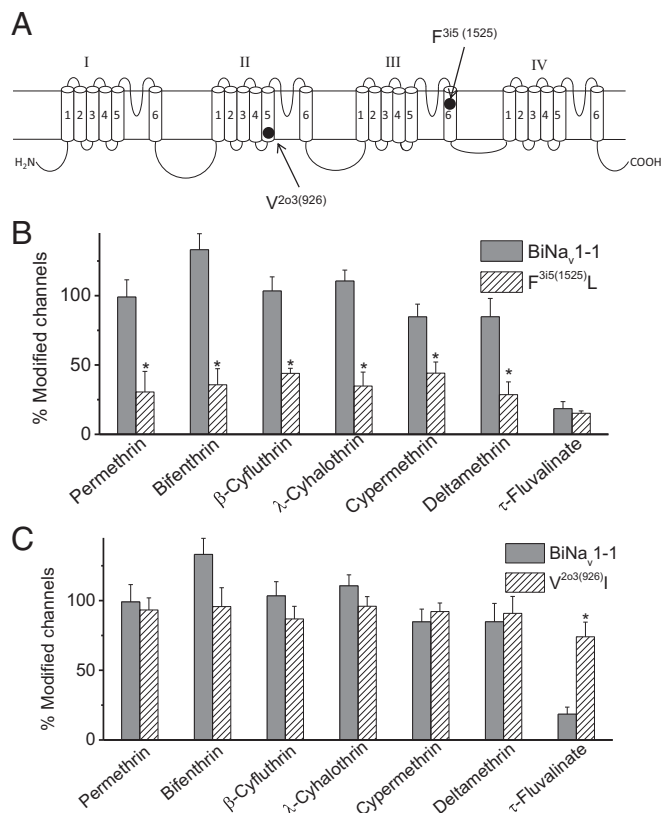

Fig. 2. Effect of mutations on the sensitivity of the $BiNa_v1–1$ channel to pyrethroids. (*A*) Position of $F^{3i5(1525)}$ and $V^{2o3(926)}$ in the topology of insect sodium channels. (*B*) The $F^{3i5(1525)}$L substitution reduced the sensitivity of the $BiNa_v1–1$ channel to permethrin, bifenthrin, β-cyfluthrin, λ-cyhalothrin, cypermethrin, and deltamethrin, but not to τ-FVL. (*C*) Substitution $V^{2o3(926)}$ I enhanced the sensitivity of the $BiNa_v1–1$ channel to τ-FVL. Percentage of modification of wild-type or mutant $BiNa_v1–1$ sodium channels by pyrethroids (1 μM) was determined using the method by Tatebayashi and Narahashi (24). The number of oocytes for wild-type and mutant channels was >5. Error bars indicate mean ± SEM. Asterisks indicate significant differences between wild-type and mutant channels, as determined by one-way analysis of variance with Scheffé's post hoc analysis, and significant values were set at *P* < 0.05.

The latter is a known pyrethroid-sensing residue, which is far from F^{3i5}. We explored two possible orientations of DMT in which the 2,2-dibromoviny moiety and terminal aromatic ring were constrained, respectively, either to F^{3i5} and M^{2k11} or to M^{2k11} and F^{3i5}. We performed Monte Carlo minimizations with the distance constraints, then removed the constraints and submitted another Monte Carlo energy minimization trajectory to refine the energetically preferable binding modes. According to our calculations, both orientations are energetically possible. We focused on the DMT binding mode (Fig. 4*A*), in which the bromine atoms were attracted by π-electrons of F^{3i5} (36). The ligand was within 5 Å from 13 residues in the four helices, which were previously proposed to contribute to the PyR1 site (26): one residue in the linker helix IIL45 (M^{2k11}), four residues in the helix IIS5 (V^{2o3}, L^{2o6}, T^{2o10}, and C^{2o14}), three residues in repeat II inner helix IIS6 (V^{2i18}, F^{2i21}, and L^{2i25}), and five residues in repeat III inner helix IIIS6 (F^{3i5}, V^{3i8}, I^{3i12}, F^{3i13}, and F^{3i16}). These residues (except for V^{2o3}, F^{3i5}, and V^{3i8}) also contribute to our $K_v1.2$-based model of PyR1 (26). In this DMT binding mode, the bulky dimethylcyclopropyl moiety fit the hydrophobic II/III fenestration, bromine atoms were attracted by F^{3i5}, and the nitrile group accepted an H-bond from T^{2o10}.
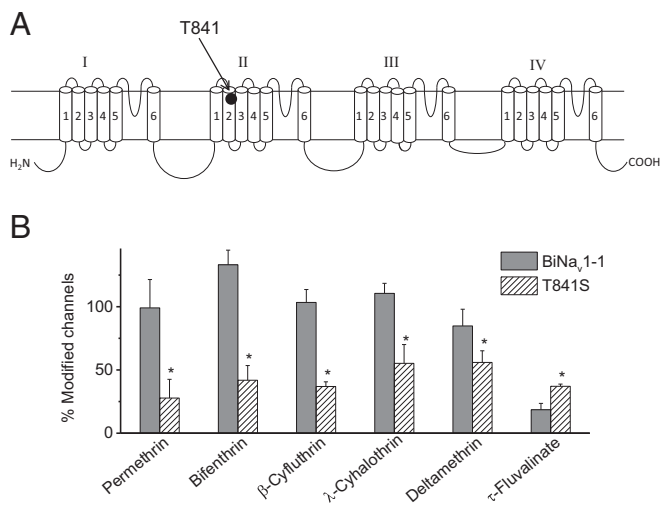
Fig. 3. Substitution T841S enhanced the sensitivity of the BiNa$_v$1–1 channel to τ-FVL. (*A*) Position of T841 in the topology of insect sodium channels. (*B*) Percentage of modification of wild-type and mutant BiNa$_v$1–1 sodium channels by pyrethroids (1 μM). The number of oocytes for wild-type and mutant channels was >5. Error bars indicate mean ± SEM. Asterisks indicate significant differences between wild-type and mutant channels, as determined by one-way analysis of variance with Scheffé's post hoc analysis, and significant values were set at *P* < 0.05.

DMT and τ-FVL have a common end (alpha-cyano-3-phenoxybenzyl moiety; Fig. S3). However, the carbonyl carbon in DMT and τ-FVL is separated from the halogen atom by five and eight bonds, respectively, implying that in the extended conformation, τ-FVL is much longer that DMT. We docked τ-FVL with the terminal aromatic ring directed to M^{2k11} (Fig. 4*B*). The ligand was within 5 Å from most of the DMT-sensing residues, but did not approach F^{3i5}, likely because π-electrons electrostatically repelled the CF$_3$ group (37). τ-FVL was also close to I^{2o17}, where a pyrethroid-resistant knockdown mutation I^{2o17}V has been found in esfenvalerate-resistant pollen beetle populations (38).

Identification of Additional Residues in PyR1 and PyR2 Affecting the BiNa$_v$1–1 Channel Sensitivity to τ-FVL. To further investigate the molecular basis of the differential sensitivity of the BiNa$_v$1–1 channel to τ-FVL vs. other pyrethroids, we generated alanine substitutions of two residues in IIIS6, V^{3i8}, and S^{3i15}. V^{3i8} is within 5 Å of PyR1-bound τ-FVL (Fig. 4*B*). We reasoned that mutation S^{3i15}A may eliminate a possible helix-bending H-bond

of S^{3i15} with the backbone carbonyl (39), and thus affect conformation of IIIS6 that contains several pyrethroid-sensing residues. Strikingly, both V^{3i8}A and S^{3i15}A mutations enhanced the BiNa$_v$1–1 channel sensitivity to τ-FVL (Fig. 5*B*), but did not alter the channel sensitivity to DMT, permethrin, bifenthrin, β-cyfluthrin, or λ-cyhalothrin.

As described earlier, the differential sensitivity of BiNa$_v$1–1 to τ-FVL vs. other pyrethroids was affected by alanine substitutions of F^{3i5} and V^{3i8}, which are located within PyR1, and S^{3i15}, which is close to PyR1. Analogous positions within or close to PyR2 harbor P^{2i5}, L^{2i8}, and N^{2i15}, respectively. To investigate possible role of these residues in the differential selectivity of BiNa$_v$1–1 to τ-FVL vs. other pyrethroids, we have made the following mutations: P^{2i5}F, L^{2i8}A, and N^{2i15}A. We found that mutation P^{2i5}F, which may have a larger effect on the ligand binding to PyR2 than mutations P^{2i5}A, significantly enhanced the BiNa$_v$1–1 channel sensitivity to τ-FVL, but not to permethrin, bifenthrin, or λ-cyhalothrin (Fig. 5*C*). The N^{2i15}A substitution also enhanced the sensitivity of BiNa$_v$1–1 to τ-FVL, but reduced the sensitivity to the other pyrethroids (Fig. 5*C*). The L^{2i8}A substitution reduced the sensitivity of BiNa$_v$1–1 only to permethrin and bifenthrin (Fig. 5*C*). These results suggest that, unlike most pyrethroids, τ-FVL lacks strong interactions with PyR1 and PyR2 in the wild-type BiNa$_v$1–1 channel.

Our mutational and computational analyses prompted us to hypothesize that the extended length of τ-FVL may interfere with its binding to the pyrethroid receptor sites in the bumblebee sodium channel, but not other insect sodium channels. To test this hypothesis, we explored the action of another relatively long pyrethroid, etofenprox (Fig. S9*A*). We found that the BiNa$_v$1–1 channel is indeed resistant to etofenprox, in contrast to sodium channels from the German cockroach (*B. germanica*), the fruit fly (*D. melanogaster*), and the yellow fever mosquito (*Ae. aegypti*), which are more sensitive to etofenprox (Fig. S9*B*). We further docked etofenprox into the PyR1 site and arrived to the binding mode resembling that of τ-FVL (Fig. S9*C*). Unlike DMT, Both τ-FVL and etofenprox extend all along the lipid-facing side of fenestration in the II/III repeat interface from the IIL45 linker helix to the IIP1 helix (Fig. 4*B* and Fig. S9*C*).

Discussion

In this study, we discovered that the sodium channel BiNa$_v$1–1 from the common eastern bumblebee is hypersensitive to six commonly used pyrethroids, but is selectively resistant to τ-FVL. Our molecular and functional characterization of the BiNa$_v$1–1 channel uncovered seven key residues, F^{3i5}, V^{2o3}, P^{2i5}, N^{2i15}, V^{3i8}, S^{3i15}, and T841 (in IIS2; Fig. 5*A* and Table S3), that are
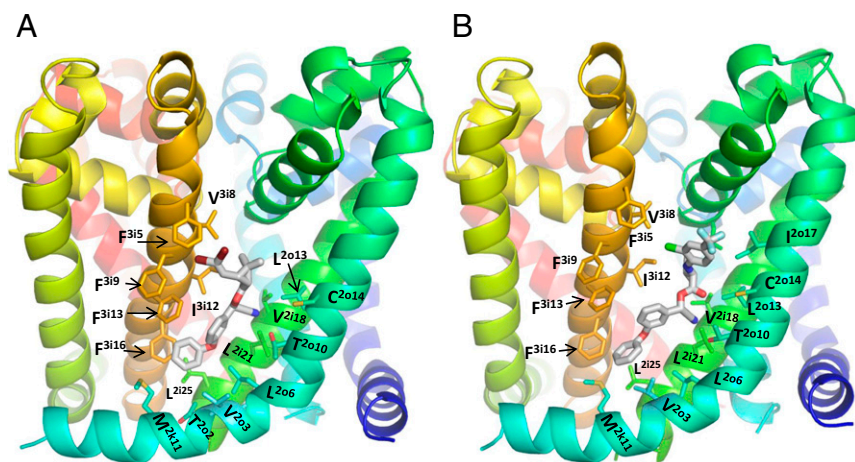

Fig. 4. A NavMs-based model of the open BiNa$_v$1–1 channel with PyR1-bound ligands DMT (*A*) and τ-FVL (*B*). Helices are blue in repeat I, green/cyan in repeat II, yellow/orange in repeat III, and red in repeat IV. Residues in the IIL45, IIS5, IIS6, and III6 helices, which are within 5 Å from the ligands are shown by sticks. In both ligands, the terminal phenyl ring, a fingerprint of pyrethroids, fits between helices IIIS6 and IIL45. Bulky hydrophobic moiety (dimethylcyclopyl in DMT and isopropyl in τ-FVL), another fingerprint of pyrethroids, fits the membrane-side entry into the fenestration, which is lined by hydrophobic residues. Bromine atoms of DMT approach F^{3i5} and would be electrostatically attracted by π-electrons. In contrast, the trifluoromethyl group of τ-FVL is far from F^{3i5}. The pore-facing S^{3i15} (not shown) is also far from τ-FVL. Mutation S^{3i15}A may eliminate a helix-bending H-bond. This may reshape IIIS6, thus allosterically affecting the τ-FVL action.
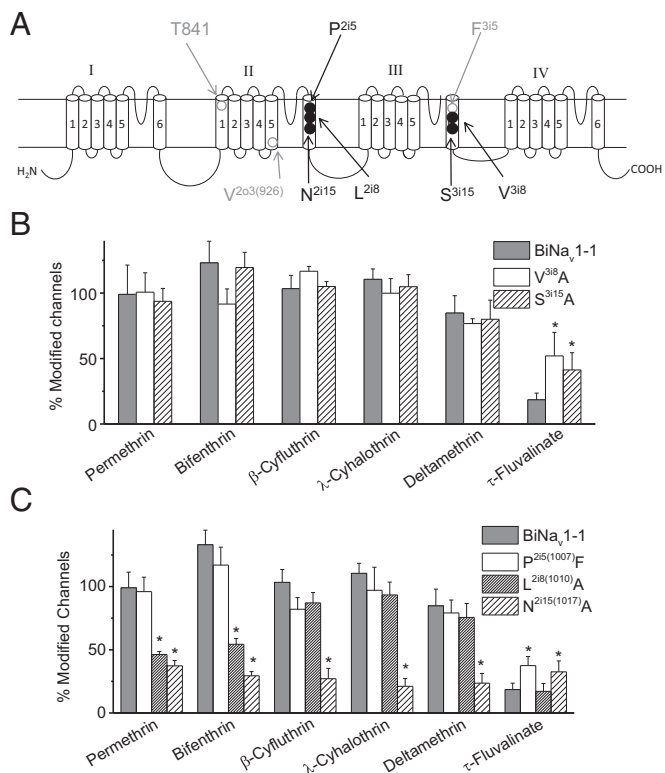
Fig. 5. Substitutions of residues in PyR1 and PyR 2 enhanced the sensitivity of the $BiNa_v1$–1 channel to τ-FVL. (*A*) Positions of relevant residues in the topology of insect sodium channels. The three bee-specific residues (Figs. 3 and 4) are also indicated using empty circles. (*B* and *C*) Effects of mutations in PyR1 (*B*) and in PyR2 (*C*) on the sensitivity of $BiNa_v1$–1 channels to pyrethroids (1 μM). The number of oocytes for wild-type and mutant channels was >5. Error bars indicate mean ± SEM. Asterisks indicate significant differences between wild-type and mutant channels as determined by one-way analysis of variance with Scheffé's post hoc analysis, and significant values were set at $P < 0.05$.

responsible for the sensitivity of bumblebees to the majority of pyrethroids and selective resistance to τ-FVL. Our study provides insight into a long-standing enigma of selective pyrethroid toxicity in bee species.

F^{3i5} and V^{2o3} are close to previously discovered pyrethroid-sensing residues within the PyR1 site (26, 29). Our experimental and molecular modeling data suggest that F^{3i5} and V^{2o3} in $BiNa_v1$–1 concertedly form favorable contacts with DMT, but unfavorable contacts with τ-FVL and etofenprox. One possibility is that the extended ligand does not fit between F^{3i5} and V^{2o3}, and deviates from F^{3i5}, and thus loses some contacts with IIIS6. Intriguingly, mutation V^{2o3}I increases the τ-FVL potency (Fig. 2*C*). Isoleucine in the V^{2o3}I mutant may either provide additional contact (methyl group) to τ-FVL or adopt a sidechain conformation that would give more room for the long ligand. Our NavMs-based homology model of the asymmetric eukaryotic channel is not precise enough to determine between these possibilities.

The binding mode of DMT in PyR1 with its 2,2-dibromovinyl group interacting with F^{3i5} is different from two previously proposed models (26, 29). However, the overall orientation of DMT in the II/III interface resembles the first model (29) more than the second model (26). In the open-sodium channel template, NavMs, which has become available only recently (32), the subunit interfaces (fenestrations) are much wider than in K_v1.2-based models (30), which were used before to elaborate both of the previous sodium channel models of pyrethroid binding (26, 29). The hydrophobic fenestration between repeats II and III is wide enough to accommodate the bulky hydrophobic moieties

(dimethylcyclopropyl in DMT, isopropyl in τ-FVL, or dimethyl-methylene in etofenprox), which seem to be an important fingerprint of pyrethroids. Substitutions V^{2o3}I, V^{3i8}A, and S^{3i15}A in PyR1, and P^{2i5}F and N^{2i15}A in PyR2, enhanced the sensitivity of the $BiNa_v1$–1 channel to τ-FVL, but not to the other pyrethroids (Table S3). These results indicate that the resistance of the $BiNa_v1$–1 channel to τ-FVL is likely a result of weak binding of τ-FVL at the PyR1 and PyR2 sites in the $BiNa_v1$–1 channel. The structural features of τ-FVL prevent its proper interactions within PyR1 and PyR2 in the wild-type $BiNa_v1$–1 channel. Further computer modeling will be needed to explore how the above substitutions may enhance the action of τ-FVL on bee sodium channels.

Except for the bee-specific F^{3i5} and V^{2o3}, all other residues contributing to PyR1 and PyR2 are conserved among sodium channels from all insect species for which the sodium channel sequence is known. Accordingly, we suggested that residues outside the identified pyrethroid receptor sites may allosterically affect the interaction of τ-FVL with the pyrethroid binding sites. Such receptor site-independent mechanisms of pyrethroid resistance have been reported previously (40, 41). Indeed, our experimental data show that T841 is such a unique residue in bee sodium channels that contributes to τ-FVL resistance. Reduced sensitivity to τ-FVL was observed when a threonine was replaced by serine at the corresponding position in the cockroach sodium channel BgNa$_v$1–1a. T841 is located in helix IIS2 of the second-repeat voltage-sensing domain, far from the pyrethroid receptor sites PyR1 and PyR2 in the II/III and I/II repeat interfaces (fenestrations) of the pore domain (26). At the corresponding position of IIS2, a serine is found in BgNa$_v$1–1 and other sodium channels from nonhymenoptera insect species. Mutation T841S did not alter the voltage dependence of gating (Table S1) and likely indirectly affected the τ-FVL action through conformational changes in the pore domain.

Recently, Gosselin-Badaroudine and Chahine (17) reported that the sodium channel AmNa$_v$1 from the honeybee (*A. mellifera*) was more sensitive to τ-FVL than to permethrin and fenvalerate, a type II pyrethroid (13, 17). Furthermore, the AmNa$_v$1 channel was also more sensitive to τ-FVL than a sodium channel variant from varroa mites (17). These results do not concur with our findings, suggesting the contribution of pyrethroid sensitivity of sodium channels to in vivo toxicity of these compounds could be different between honeybees and bumblebees (42–44).

Our study provided an example of a sodium channel that displays a striking selective resistance to an insecticide, which is widely used in the control of agricultural pests and varroa mites. One unique structural feature of τ-FVL is its extended length. Our mutational and computational analyses suggest the long τ-FVL does not fit pyrethroid receptor sites in the bumblebee sodium channel well, but fits those in other insect sodium channels. We have tested this hypothesis using etofenprox, which in the extended conformation is at least as long as τ-FVL (Fig. S8). Our experiments showed that, similar to τ-FVL, etofenprox was also selectively less potent to BiNa$_v$ channels than to other insect sodium channels. We hope that our study could encourage more effort on future knowledge-based precise modification of pyrethroids to achieve a new generation of highly selective control of pests with minimal effects on nontarget beneficial insect species, including bees.

Materials and Methods

Isolation of a Full-Length BiNav1–1 cDNA Clone by RT-PCR. Total RNA was isolated from the brains of adult bumblebees (*B. impatiens*) using the Invitrogen TRIzol Reagent kit (Invitrogen). Procedures for first-strand cDNAs, PCR and cloning of the full-length BiNa$_v$ cDNA were similar to those described by Olson et al. (20). The entire coding region was amplified by RT-PCR, using primers 5′-CCGCCCGGGGCCACCATGGCCGAAGATTCTGACTCTGT-ATCA-3′ (forward primer) and 5′-CCCAAGCTTGCGGTGCTTGGGACGTCGTG-GACG-3′ (reverse primer). The PCR product was cloned into pGH19, a *Xenopus* oocyte expression vector. A full-length clone was isolated and sequenced in the Research Technology Support Facility at Michigan State University.

Site-Directed Mutagenesis. Site-directed mutagenesis was performed by PCR, using mutant primers and Phusion High-Fidelity DNA Polymerase (NEB). All mutagenesis results were verified by DNA sequencing.

Expression of BiNa$_v$1–1 Sodium Channels in *Xenopus* oocytes and Electrophysiological Analysis. Procedures for oocyte preparation, cRNA synthesis, and injection into oocytes were identical to those described previously (21). For robust expression, BiNa$_v$1–1, AaNa$_v$1–1, and BgNa$_v$1–1a cRNA was coinjected into oocytes with corresponding *TipE* cRNA (at a 1:1 molar ratio). Methods for electrophysiological recording and data analysis were similar to those described previously (45). The methods for application of pyrethroids in the recording system and measurement of tail currents induced by pyrethroids were identical to those described previously (21).

Insecticides. Insecticides used in this study (Fig. S3) were purchased from Sigma-Aldrich except for (1R)-cis-permethrin, which was purchased from Chem Service. All insecticides used were of technical grade (>95% purity).

Molecular Modeling. We used a recent X-ray structure of the open bacterial channel, NavMs (32), to build a homology model of the BiNa$_v$1–1 channel and docked DMT, τ-FVL, and etofenprox, in the PyR1 site. The docking methodology with the ZMM program was described elsewhere (26, 35). We have designated residues (Table S4) using a nomenclature that is universal for P-loop channels (19, 28).

1. Oldroyd BP (2007) What's killing American honey bees? *PLoS Biol* 5:e168.
2. Goulson D (2010) *Bumblebees: Behaviour, Ecology, and Conservation* (Oxford Univ Press, Oxford).
3. Delaplane KS, Mayer DR, Mayer DF (2000) *Crop Pollination by Bees* (CABI Publishing, Cambridge, MA).
4. Velthuis HH, Van Doorn A (2006) A century of advances in bumblebee domestication and the economic and environmental aspects of its commercialization for pollination. *Apidologie* 37:421–451.
5. Colla SR, Gadallah F, Richardson L, Wagner D, Gall L (2012) Assessing declines of North American bumble bees (Bombus spp.) using museum specimens. *Biodivers Conserv* 21:3585–3595.
6. Kerr JT, et al. (2015) Climate change impacts on bumblebees converge across continents. *Science* 349:177–180.
7. Williams PH, Osborne JL (2009) Bumblebee vulnerability and conservation worldwide. *Apidologie* 40:367–387.
8. Goulson D, Lye GC, Darvill B (2008) Decline and conservation of bumble bees. *Annu Rev Entomol* 53:191–208.
9. Cameron SA, et al. (2011) Patterns of widespread decline in North American bumble bees. *Proc Natl Acad Sci USA* 108:662–667.
10. Casida JE, Durkin KA (2013) Neuroactive insecticides: Targets, selectivity, resistance, and secondary effects. *Annu Rev Entomol* 58:99–117.
11. Sanchez-Bayo F, Goka K (2014) Pesticide residues and bees–A risk assessment. *PLoS One* 9:e94482.
12. Sterk GM, Kolokytha PD (2015) New insights of side-effects of tau-fluvalinate on biologica agents and pollinators. *Commun Agric Appl Biol Sci* 80:65–70.
13. Gosselin-Badaroudine P, et al. (2015) Characterization of the honeybee AmNaV1 channel and tools to assess the toxicity of insecticides. *Sci Rep* 5:12475.
14. Kadala A, et al. (2014) Pyrethroids differentially alter voltage-gated sodium channels from the honeybee central olfactory neurons. *PLoS One* 9:e112194.
15. Kadala A, Charreton M, Jakob I, Le Conte Y, Collet C (2011) A use-dependent sodium current modification induced by type I pyrethroid insecticides in honeybee antennal olfactory receptor neurons. *Neurotoxicology* 32:320–330.
16. Zhou T, et al. (2011) Effects of pyrethroids on neuronal excitability of adult honeybees Apis mellifera. *Pestic Biochem Physiol* 100:35–40.
17. Gosselin-Badaroudine P, Chahine M (2017) Biophysical characterization of the Varroa destructor NaV1 sodium channel and its affinity for τ-fluvalinate insecticide. *FASEB J* 31:3066–3071.
18. Santiago GP, Otero-Colina G, Sanchez DM, Guzman MER, Vandame R (2000) Comparing effects of three acaricides on Varroa jacobsoni (Acari: Varroidae) and Apis mellifera (Hymenoptera: Apidae) using two application techniques. *Fla Entomol* 83:468–476.
19. Du Y, et al. (2013) Molecular evidence for dual pyrethroid-receptor sites on a mosquito sodium channel. *Proc Natl Acad Sci USA* 110:11785–11790.
20. Olson RO, Liu Z, Nomura Y, Song W, Dong K (2008) Molecular and functional characterization of voltage-gated sodium channel variants from *Drosophila melanogaster*. *Insect Biochem Mol Biol* 38:604–610.
21. Tan J, et al. (2002) Novel sodium channel gene mutations in *Blattella germanica* reduce the sensitivity of expressed channels to deltamethrin. *Insect Biochem Mol Biol* 32:445–454.
22. Warmke JW, et al. (1997) Functional expression of *Drosophila para* sodium channels. Modulation by the membrane protein TipE and toxin pharmacology. *J Gen Physiol* 110:119–133.
23. Vais H, et al. (2003) Mutations of the *para* sodium channel of *Drosophila melanogaster* identify putative binding sites for pyrethroids. *Mol Pharmacol* 64:914–922.
24. Tatebayashi H, Narahashi T (1994) Differential mechanism of action of the pyrethroid tetramethrin on tetrodotoxin-sensitive and tetrodotoxin-resistant sodium channels. *J Pharmacol Exp Ther* 270:595–603.
25. Lund AE, Narahashi T (1982) Dose-dependent interaction of the pyrethroid isomers with sodium channels of squid axon membranes. *Neurotoxicology* 3:11–24.
26. Du Y, Nomura Y, Zhorov BS, Dong K (2015) Rotational symmetry of two pyrethroid receptor sites in the mosquito sodium channel. *Mol Pharmacol* 88:273–280.
27. Du Y, Garden DP, Wang L, Zhorov BS, Dong K (2011) Identification of new batrachotoxin-sensing residues in segment IIIS6 of the sodium channel. *J Biol Chem* 286:13151–13160.
28. Zhorov BS, Tikhonov DB (2004) Potassium, sodium, calcium and glutamate-gated channels: Pore architecture and ligand action. *J Neurochem* 88:782–799.
29. O'Reilly AO, et al. (2006) Modelling insecticide-binding sites in the voltage-gated sodium channel. *Biochem J* 396:255–263.
30. Long SB, Campbell EB, Mackinnon R (2005) Crystal structure of a mammalian voltage-dependent Shaker family K+ channel. *Science* 309:897–903.
31. Lenaeus MJ, et al. (2017) Structures of closed and open states of a voltage-gated sodium channel. *Proc Natl Acad Sci USA* 114:E3051–E3060.
32. Sula A, et al. (2017) The complete structure of an activated open sodium channel. *Nat Commun* 8:14205.
33. Shen H, et al. (2017) Structure of a eukaryotic voltage-gated sodium channel at near-atomic resolution. *Science* 355:eaal4326.
34. Tikhonov DB, Zhorov BS (2017) Mechanism of sodium channel block by local anesthetics, antiarrhythmics, and anticonvulsants. *J Gen Physiol* 149:465–481.
35. Garden DP, Zhorov BS (2010) Docking flexible ligands in proteins with a solvent exposure- and distance-dependent dielectric function. *J Comput Aided Mol Des* 24:91–105.
36. Matter H, et al. (2009) Evidence for C-Cl/C-Br...pi interactions as an important contribution to protein-ligand binding affinity. *Angew Chem Int Ed Engl* 48:2911–2916.
37. Katagiri T, Yamaji S, Handa M, Irie M, Uneyama K (2001) Diastereoselectivity controlled by electrostatic repulsion between the negative charge on a trifluoromethyl group and that on aromatic rings. *Chem Commun (Camb)* 2054–2055.
38. Wrzesińska B, et al. (2014) A survey of pyrethroid-resistant populations of Meligethes aeneus F. in Poland indicates the incidence of numerous substitutions in the pyrethroid target site of voltage-sensitive sodium channels in individual beetles. *Insect Mol Biol* 23:682–693.
39. Chakrabartty A, Kortemme T, Baldwin RL (1994) Helix propensities of the amino acids measured in alanine-based peptides without helix-stabilizing side-chain interactions. *Protein Sci* 3:843–852.
40. Du Y, et al. (2010) A negative charge in transmembrane segment 1 of domain II of the cockroach sodium channel is critical for channel gating and action of pyrethroid insecticides. *Toxicol Appl Pharmacol* 247:53–59.
41. Oliveira EE, Du Y, Nomura Y, Dong K (2013) A residue in the transmembrane segment 6 of domain I in insect and mammalian sodium channels regulate differential sensitivities to pyrethroid insecticides. *Neurotoxicology* 38:42–50.
42. Arena M, Sgolastra F (2014) A meta-analysis comparing the sensitivity of bees to pesticides. *Ecotoxicology* 23:324–334.
43. Cresswell JE, et al. (2012) Differential sensitivity of honey bees and bumble bees to a dietary insecticide (imidacloprid). *Zoology (Jena)* 115:365–371.
44. Rinkevich FD, et al. (2015) Genetics, synergists, and age affect insecticide sensitivity of the honey bee, Apis mellifera. *PLoS One* 10:e0139841.
45. Tan J, et al. (2005) Identification of amino acid residues in the insect sodium channel critical for pyrethroid binding. *Mol Pharmacol* 67:513–522.
46. Dong K, et al. (2014) Molecular biology of insect sodium channels and pyrethroid resistance. *Insect Biochem Mol Biol* 50:1–17.

AGRICULTURAL SCIENCES